

# Design and Simulation of a MEMS Long Distance Traveling Actuator

Y. Elkacimi<sup>1</sup>, N. Müller<sup>2</sup>

<sup>1</sup>Michigan State University, Department of Mechanical Engineering  
2500 Engineering Building, East Lansing, MI 48824, U.S.A.  
elkacimi@egr.msu.edu

<sup>2</sup>Michigan State University, Department of Mechanical Engineering  
2455 Engineering Building, East Lansing, MI 48824, U.S.A.  
mueller@egr.msu.edu

## Abstract

This work primarily presents the design, synthesis, modeling, and simulation of a linear micro-actuator that is able to travel relatively long distances (order of 1000  $\mu\text{m}$ ). An electrostatic force generated through the application of a bias voltage operates this actuator. An analytical study investigates the functionality of this device in a setting of given fixed and variable parameters as it can be used for realistic applications. The analysis shows that several parameters, such as the thickness, width, and length of the electrodes have a direct effect on the performance of the device.

*Keywords: PowerMEMS, Micro-actuator, Electrostatic Force, Systems-on-a-Chip, Process Flow*

## 1- INTRODUCTION

Rotational and linear micromotors are often found to be a key part of micromechanical systems allowing them to perform physical functions. They can be used for aperture or gap controlling, and as driver for micro-relays, micro-mirrors and micro-grippers amongst other applications. The concept behind the long distance traveling micro-actuator is basically an actuator operating by virtue of electrostatic force. This micro-actuator device is composed of three main parts. One component constitutes a long conductive fixed track directly attached to a nitride layer, which is deposited on the top of the main surface (Silicon substrate). The other element is a shuttle, which is a conductive carrier made out of doped polysilicon that slides over the fixed track. This shuttle has lateral poles ‘bumps’ on both opposing sides parallel to the track. The third element is a set of electrodes built on both sides of the track, in a way that would allow the bumps on the shuttle (in this case 12 poles- six on each side of the shuttle) to completely overlap with some of the fixed electrodes at any given time, and partially overlap with others as shown in Fig. 1. This design will allow the shuttle to move (slide) over the track (Fig. 2) upon the application of a bias voltage.

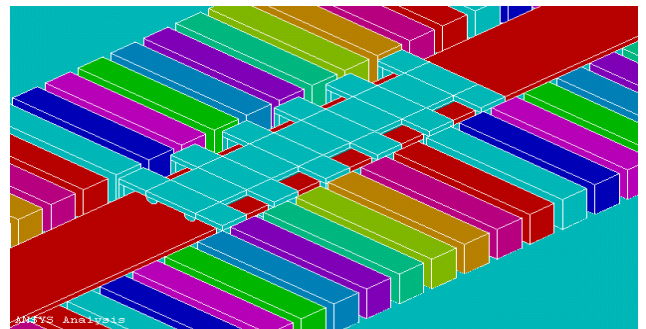


**Figure 1** - A solid 3D drawing of the linear microactuator drawn to scale

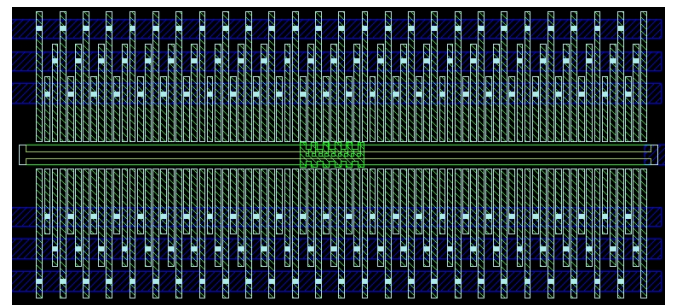


**Figure 2** - Mentor Graphic image of part of the device (the track, shuttle, and fixed electrodes) showing all the layers of the different masks.

## 2 - PRINCIPLE OF OPERATION

The concept of operation of the long range traveling laterally operated electrostatically driven micro-actuator is somewhat similar to that of a synchronous side drive motor. The sliding anchor (shuttle) is set between two sets of opposing stator electrodes (Fig. 1). The stator poles and sliding poles (shuttle poles) are laid out in a fashion, which allows a few of the stator poles to be completely overlapping with other poles on the sliding anchor. The stator electrodes and the sliding poles are charged and move the anchor by tangential electrostatic force as long as the electrode faces remain shifted. When the faces stand opposite to each other, the next stator electrodes are charged and so on.

### 2.1 - Actuation Principle

The right choice of the actuation principle is dependent on the structural dimensions, the technology, the response time, the force as a function of displacement, the maximum power consumption, and other factors as well. In this work, electrostatic-based actuation is opted for, because it combines versatility and simple technology, and because of its compatibility with micromachining, such as surface micromachining technology for which the process flow is designed in this study. Electrostatic actuation needs neither additional elements like coils or cores, as it is the case for electromagnetic actuators, nor special materials like shape-memory-alloys or piezoelectric ceramics. The electrostatic actuation draws its force from the relation of surface to spacing and not from the relation of volume to spacing [1].

### 2.2 - Excitation Scheme

The conventional excitation sequence consists of successive activation of three partially overlapped terminals (one phase). The electrodes structures are operated with 3-phase circuit capable of output voltages from 5 to 30 volts with frequencies  $f_o$  (Fig. 3) ranging from 183.3 KHz to 1860 KHz respectively. The values obtained for these frequencies are based on the periods (time to perform one cycle) calculated corresponding to the distance covered by the partially overlapping poles from one phase to the other. This distance covered is set to be 6 microns by design. The speed with which the phases change from one to the other depends on the magnitude of the voltage applied.

## 3 - MATHEMATICAL MODEL

A force-based approach was taken to create a mathematical model for the laterally driven linear microactuator. This approach is used to calculate the static device behavior by considering the balance between the attractive electrical force and any elastic restoring forces. All the external forces, which have a noticeable effect were determined and included to develop an equation of motion for the microsystem. A structural equation was developed to predict the actuator position as a function of applied voltage, and define the stable, low voltage region of operation prior to runaway or pull-in, where the nonlinear electrostatic force overcomes the typically linear restoring force, or the forces impeding the motion

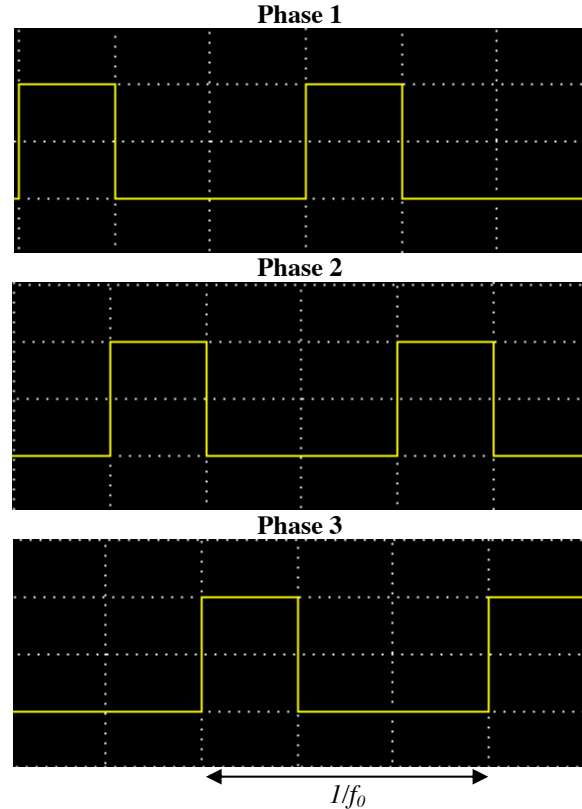


Figure 3 - Excitation Scheme for Linear Motion of the Microactuator

### 3.1 - Mechanical System

The main body of the electrostatic microactuator can be modeled as a classical second order mechanical system with a single degree-of-freedom. The force responsible for the motion of the shuttle is the electrostatic force  $F_e$  generated by the bias voltage. The shuttle, being the moving part in this microsystem (Fig. 4), is situated on the top of, and therefore touching, the fixed track by means of ‘dimples’, which were designed to minimize surface friction between the shuttle and its support.

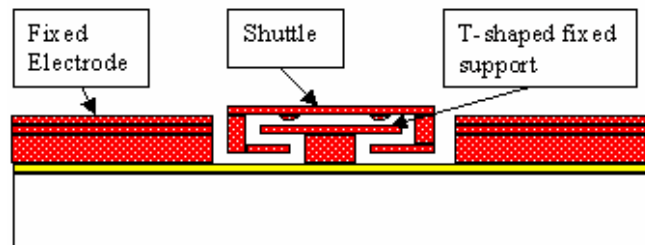


Figure 4 - Schematic of the Cross sectional Area of the linear Actuator

The contact of the shuttle and the T-shaped support is cause for dry friction force (or coulomb force)  $F_C$ , which works to impede the motion of the transport. Since this device is designed to operate in air under normal room temperature and

atmospheric conditions, the drag force  $F_D$  is, thus, another external force the shuttle is being subjected to.

$$F_D = \frac{1}{2} C_D \cdot \rho \cdot A \cdot (x')^2 \quad (1)$$

$$F_C = \mu_k \cdot m \cdot G \cdot \text{sgn}(x') \quad (2)$$

$$F_e = \frac{n}{2} \cdot \varepsilon_0 \cdot \varepsilon_r \cdot \frac{h}{d} \cdot V^2 \quad (3)$$

The differential equation of motion of this forced second order mechanical system is given by:

$$m \cdot x'' + \frac{1}{2} C_D \cdot \rho \cdot A \cdot (x')^2 = \frac{n}{2} \cdot \varepsilon_0 \cdot \varepsilon_r \cdot \frac{h}{d} \cdot V^2 - \mu_k \cdot m \cdot G \cdot \text{sgn}(x') \quad (4)$$

Solving it, gives expressions for velocity and displacement:

$$x' = \frac{\sqrt{D}}{\sqrt{P}} \cdot \frac{(C' \cdot e^{\theta \cdot t} - 1)}{(C' \cdot e^{\theta \cdot t} + 1)} \quad (5)$$

$$x = \frac{2 \cdot \sqrt{D}}{\theta \cdot \sqrt{P}} \cdot \ln(\sqrt{P} + \sqrt{P} \cdot C' \cdot e^{\theta \cdot t}) - \frac{\sqrt{D}}{\sqrt{P}} \cdot (t) \quad (6)$$

where

$$P = \frac{1}{2} C_D \cdot \rho \cdot A$$

$$D = \frac{n}{2} \cdot \varepsilon_0 \cdot \varepsilon_r \cdot \frac{h}{d} \cdot V^2 - \mu_k \cdot m \cdot G$$

$$C = e^{\left[ c_3 - \frac{(c_1 + c_2)}{2 \cdot \sqrt{D}} \right]}$$

$$q = \frac{1}{2 \cdot \sqrt{P} \cdot D} \quad C' = C^q \quad \theta = \frac{1}{m \cdot q}$$

Using boundary conditions,  $C'$  is determined:

$$C' = \frac{1 - \sqrt{P}}{\sqrt{P}}$$

The expressions for the displacement and velocity become:

$$x(t) = \frac{m}{P} \cdot \ln \left[ \sqrt{P} + (1 - \sqrt{P}) \cdot e^{\left( 2 \cdot \frac{\sqrt{P} \cdot D}{m} \right) \cdot t} \right] - \frac{\sqrt{D}}{\sqrt{P}} \cdot (t) \quad (7)$$

$$x' = \frac{\sqrt{D}}{P} \cdot \frac{\left[ (1 - \sqrt{P}) \cdot e^{\left( 2 \cdot \frac{\sqrt{P} \cdot D}{m} \right) \cdot t} - \sqrt{P} \right]}{\left[ (1 - \sqrt{P}) \cdot e^{\left( 2 \cdot \frac{\sqrt{P} \cdot D}{m} \right) \cdot t} + \sqrt{P} \right]} \quad (8)$$

### 3.2 - Other Forces

Friction forces and stiction have been considered in the model. Doped polysilicon, as deposited and used in the model, shows relatively high friction (0.07), which is due to the presence of grain boundaries and high surface roughness [4]. However, polishing of the doped polysilicon film results in very low coefficient of friction (0.02).

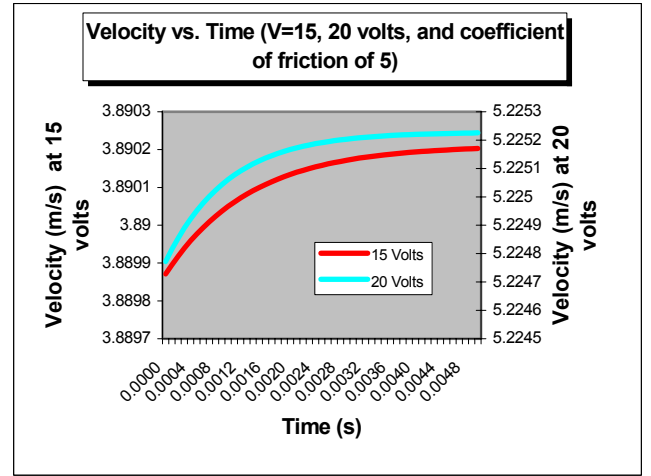


**Figure 5** - Velocity of the Shuttle vs. Time using a Kinetic friction coefficient of 0.05 and a voltage values of 15 and 20 volts for the time interval of [0, 5 ms].

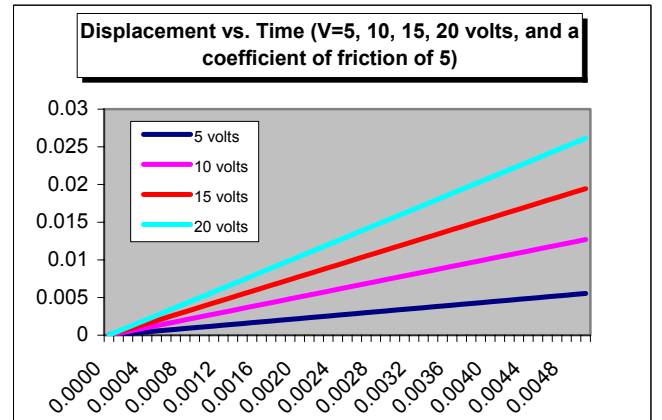


**Figure 6** - Displacement (in m) of the Shuttle vs. Time using a kinetic friction coefficient of 0.05 and a voltage values of 5, 10, 15, and 20 volts for the time interval of [0, 5 ms].

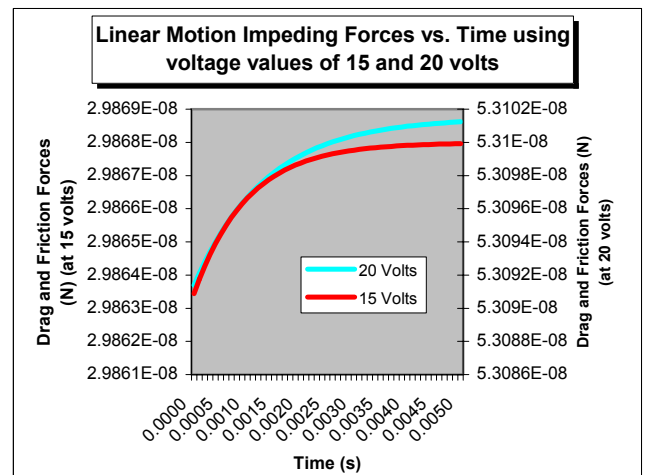


**Figure 7**: Drag and friction forces as a function of time for voltage values of 5, and 10 volts.

In the modeling of this statically driven linear microactuator, the electromagnetic forces and their effects have been ignored, because the device's surface area to volume ratio is large (3 orders of magnitude). As a result, the magnitudes of the forces, which are proportional to volume, such as electromagnetic forces become much smaller in comparison to the forces, which are proportional to the surface area. The van der Waals forces between two contacting surfaces are in many cases hard to be distinguished from electrostatic forces [5], and thus have been accounted for in the coulombic force. At the silicon-to-silicon gap of 2 microns (smallest gap used in the current design), the breakdown voltage is about 350 volts [6], which is a much higher than the voltage used in this current design (5–30 Volts). The breakdown voltage is, therefore not an issue in the current design.

#### 4 - EFFECTS OF DEVICE OPERATION

Assuming a relatively long (100 $\mu$ m-10mm) track for the shuttle to travel on, the following graphs of displacement and velocity show the behavior of the device on a range of tens of a millimeter for study of the overall behavior of the device. However some of the applications of this electrostatically driven linear microactuator may require shuttle tracks of several millimeters length.

At relatively low voltage values, the shuttle moves a distance of about 1000 microns in a few milliseconds (Fig. 6) as expected from such a device under normal operation conditions. When the shuttle is stationary, and after the voltage is applied, the electrostatic force builds up to a value that allows it to overcome static friction. After such a point, the shuttle starts moving and the frictional resistance decreases, which it, generally, does. Then the kinetic frictional resistance stays about constant, and so does the velocity. The acceleration becomes null and the device reaches a state of dynamic equilibrium (Fig. 5).

The main forces impeding the motion of the shuttle while it is traveling on the track are the dry friction and the drag forces. Figure 7 illustrates the predicted development of these forces during the shuttle's travel on the track. Even at low voltages (e.g. 15 volts) the electrostatic force moving the shuttle remains dominant, and capable of overcoming the static friction, the dry friction, and drag forces.

#### 5 - DISCUSSIONS AND CONCLUSIONS

All the significant forces exerted on this device and all the variables and parameters, which describe the environment and conditions in which this device is to be simulated in, have been considered and incorporated in the dynamic modeling of the device. Magnetic forces and fringing fields were neglected, because they were insignificant in comparison to electrostatic forces generated. Friction between the rough surfaces in contact has been assumed to have the largest kinetic coefficient as a worst-case scenario to be studied in the dynamic modeling of the device. Therefore, for all the calculations performed a value of 0.05 (highest) for the kinetic friction coefficient was used. Under ambient conditions of pressure and temperature, and for a bias voltage

of 5-30 volts enough electrostatic force is generated to overcome the friction and drag forces and to propel the device. By design, continuous motion of the shuttle is pragmatic when a three-phase voltage driver is used to power the device. The displacement of the shuttle linearly increases with time, and the shuttle travels a distance of about 1000 microns (length of the designed track) in a few milliseconds. The lowest and highest values for the velocity calculated are 1.10 m/s, and 11.16 m/s respectively, achieved with 5 and 30 volts respectively. These speeds are typical of linear micro actuators operating with comparable voltage values. For any application of such a device where carrying a load is important, larger voltages need to be applied to move the shuttle. These values can easily be determined if the weight and size of the load is known.

A manufacturing process flow was also developed and the different steps necessary to fabricate this device were studied in detail, but are not presented here.

#### ACKNOWLEDGMENTS

The authors are greatly indebted to Dr. Mustafa Abushagur from Rochester Institute of Technology for his original idea and guidance and tremendous support throughout this research. Thanks also go to Dr. Lynn Fuller, Dr. Hany Ghoneim, Dr. Edward Hensel, Dr. Alan Raisanen and others from the same institution for their advice and continuous support of this work.

#### REFERENCES

- [1] Ernst Thielicke, Ernst Obermeier. Microactuators and their technologies. Technical University of Berlin, Microsensor and Microactuator Technology Center (MAT), TIB 3.1, Gustav-Meyer-Allee 25, 13355, Berlin, Germany.
- [2] Xingtao Wu, Jiang Zhe, Jingshan Wang, Jin Cheng, Vijay Modi, and K. R. Farmer. A generalized capacitance-based model for electrostatic micro-actuators. Department of Physics, New Jersey Institute of Technology, Newark, NJ, Department of Mechanical Engineering, Columbia University, NY
- [3] Sriram Sundararajan, Bharat Bhushan. Micro/nanotribological studies of polysilicon and SiC films for MEMS applications. *Wear* 217 (1998) 251-261.
- [4] Sriram Sundararajan, Bharat Bhushan. Static friction and surface roughness studies of surface micromachined electrostatic micromotors using an atomic force/friction force microscope. January 2001.
- [5] Chih-Ming Ho, Yu-Chong Tai. Micro-Electro-Mechanical Systems (MEMS) and Fluid Flows. *Annu. Rev. Fluid Mech.* 1998. 30:579–612
- [6] M. Esashi. Silicon bulk micromachining. New Industry Creation Hatchery Center, Tohoku University, Sendai, 980-8579, Japan
- [7] Mohd P. Omar, Merhan Mehregany, Member, IEEE, and Robert L. Mullen. Electric and Fluid Analysis of Side-Drive Micromotors. *Journal of microelectromechanical systems*. VOL. 1. NO. 3. September 1992
- [8] Robert L. Mott. *Applied Fluid Mechanics*, Fifth Edition, 2000 Prentice-Hall, Inc.
- [9] John D. Anderson, Jr. *Modern Compressible Flow with Historical Perspective*, second edition. McGraw Hill, Inc. 1990
- [10] S.L. Miller, J.J. Sniegowski, G. LaVigne, and P.J. McWhorter. Friction in surface micromachined microengines. Sandia National Laboratories, Albuquerque, NM.